AGE (2013) 35:1045–1060
DOI 10.1007/s11357-012-9426-6

Identification of the dichotomous role of age-related LCK in calorie restriction revealed by integrative analysis of cDNA microarray and interactome

Daeui Park · Eun Kyeong Lee · Eun Jee Jang · Hyoung Oh Jeong · Byoung-Chul Kim · Young Mi Ha · Seong Eui Hong · Byung Pal Yu · Hae Young Chung

Received: 18 January 2012 / Accepted: 2 May 2012 / Published online: 25 July 2012

Abstract Among the many experimental paradigms used for the investigation of aging, the calorie restriction (CR) model has been proven to be the most useful in gerontological research. Exploration of the mechanisms underlying CR has produced a wealth of data. To identify key molecules controlled by aging and CR, we integrated data from 84 mouse and rat cDNA microarrays with a protein–protein interaction network. On the basis of this integrative analysis, we selected three genes that are upregulated in aging but downregulated by CR and two genes that are downregulated in aging but upregulated by CR. One of these key molecules is lymphocyte-specific protein tyrosine kinase (LCK). To further confirm this result on LCK, we performed a series of experiments in vitro and in vivo using kidneys obtained from aged ad libitum-fed and CR rats. Our major significant findings are as follows: (1) identification of LCK as a key molecule using integrative analysis; (2) confirmation that the age-related increase in LCK was modulated by CR and that protein tyrosine kinase activity was decreased using a LCK-specific inhibitor; and (3) upregulation of LCK leads to NF-κB activation in a $ONOO^-$ generation-dependent manner, which is

Electronic supplementary material The online version of this article (doi:10.1007/s11357-012-9426-6) contains supplementary material, which is available to authorized users.

D. Park · E. K. Lee · E. J. Jang · H. O. Jeong · B.-C. Kim · Y. M. Ha · H. Y. Chung
Molecular Inflammation Research Center for Aging Intervention, Pusan National University,
Busan 609-735, Republic of Korea

D. Park · H. O. Jeong · B.-C. Kim
Interdisciplinary Research Program of Bioinformatics and Longevity Science, Pusan National University,
Busan 609-735, Republic of Korea

E. K. Lee
Research Center, Dongnam Institute of Radiological and Medical Sciences,
Busan 619-953, Republic of Korea

S. E. Hong
System Biology Research Center, Gwangju Institute of Science and Technology,
Gwangju 500-712, Republic of Korea

B. P. Yu
Department of Physiology, University of Texas Health Science Center at San Antonio,
San Antonio, TX 78229-3900, USA

H. Y. Chung (✉)
Department of Pharmacy, College of Pharmacy, Pusan National University,
San 30, Jangjun-dong, Gumjung-gu,
Busan 609-735, South Korea
e-mail: hyjung@pusan.ac.kr

modulated by CR. These results indicate that LCK could be considered a target attenuated by the anti-aging effects of CR. Integrative analysis of cDNA microarray and interactome data are powerful tools for identifying target molecules that are involved in the aging process and modulated by CR.

Keywords Aging · Calorie restriction · cDNA microarray · Differentially expressed genes · Interactome · LCK

Introduction

Aging is a physiological process that is accompanied by functional decline over time. Although our knowledge of the aging process has expanded greatly in recent years, the mechanistic understanding of aging and its intervention remain a great challenge to basic science and to the medical field (Kirkwood 2005). The calorie restriction (CR) model has been proven to be the most useful probe in gerontological research. Exploration of the mechanisms underlying CR has produced a wealth of data, revealing possible clues for plausible approaches to intervene in or slow down the aging process (Yu 1996; Sinclair 2005). However, this wealth of data has led to increased complexity; understanding the mechanisms of aging and anti-aging is complicated because it is difficult to integrate and analyze separate data obtained at the cellular and organism levels.

Recent approaches have attempted to combine gene expression data with the knowledge obtained from protein–protein interaction (PPI) networks, termed the interactome. This approach allows us to analyze global gene expression changes in aging, as well as to select valuable key molecules from a large number of genes using the connections between genes. For instance, several investigators have integrated cDNA microarray and PPI networks for aging research in yeast, nematode, and fruit fly (Xue et al. 2007; Lorenz et al. 2009), and have identified longevity candidate genes and aging-related modules. However, these studies have not attempted to validate CR, which has a strong aging modulation effect in mammals. Examination of both aging and CR is a very reliable method for identifying additional effective key molecules and pathways as an approach for aging research in humans. In this study, we integrated cDNA microarray and PPI network information, demonstrating the anti-aging effect of CR based on an accumulated large-scale data compendium in mammals. Our previous study proposed a new conceptual approach to the biological processes that are modulated by aging and CR (Hong et al. 2010). In the current study, we built a transcriptome comprised of data from 84 cDNA microarrays of four different tissues underlying aging and CR based on a number of large-scale expression profiles. Using the results of microarrays, we were able to present a global view of the biological pathways governed by the aging and CR transcriptomes, and we also performed a PPI network analysis combining the graph theory for identifying key molecules among the significantly changed genes.

A series of integrative analyses have revealed that the immune response and energy metabolism are the major biological processes largely influenced by aging and CR. On the basis of an analysis of the PPI network composed of differentially expressed genes (DEGs) in aging and CR, we selected three genes that are upregulated in aging but downregulated by CR and two genes that are downregulated in aging but upregulated by CR as hubs that have high degree and centrality scores in the PPI network. Our integrative analysis suggests that one of the key molecules is LCK, which is activated by the aging process and inactivated by CR. Based on predicted results, we experimentally confirmed that the age-related increase in the expression and activity of LCK was modulated by CR and that the protein tyrosine kinase (PTK) activity was decreased by a LCK-specific inhibitor both in vitro and in vivo. These results indicate that LCK could be considered a target protein that is attenuated by anti-aging effects; LCK had not been previously identified as an important molecule in aging and CR. The integrative analysis from cDNA microarray and the interactome are very powerful tools for identifying target molecules and drugs for aging intervention.

Materials and methods

Identification of differentially expressed genes in aging and CR

We identified DEGs in aging and CR from a microarray dataset (GEO datasets, GDS) that are freely accessible in the Gene Expression Omnibus (GEO) (Table 1). We selected four datasets (a total of 84 cDNA microarrays) of kidney, skeletal muscle, heart, and white adipose tissue from mouse and rat. All datasets were generated using

Table 1 Microarray data sets tested under both aging and CR derived from GEO

GDS ID	Tissue	Animal	Description*	Up	Down
GDS355	Kidney	C57BL/6 mice	Young, 5 months, (5) vs old, 30 months, (5)	12	14
			Old, 30 months, (5) vs CR, 30 months, (5)	3	7
GDS356	Kidney	C57BL/6 mice	Young, 5 months, (5) vs old, 30 months, (5)	106	5
			Old, 30 months, (5) vs CR, 30 months, (5)	10	83
GDS2612	Skeletal muscle	C57BL/6NHsd mice	Young, 5 months, (5) vs old, 25 months, (5)	9	26
			Old, 25 months, (5) vs CR, 25 months, (5)	135	80
GDS3102	Heart	Fischer 344 rats	Young, 4 months (6) vs old, 28 months, (7)	290	62
			Old, 28 months, (7) vs CR, 28 months, (7)	0	0
	White adipose tissue	Fischer 344 rats	Young, 4 months, (7) vs old, 28 months, (5)	408	300
			Old, 28 months, (5) vs CR, 28 months, (7)	281	243

GDS IDs can be used to query the dataset in GEO (http://www.ncbi.nlm.nih.gov/geo/). () denotes the number of the cDNA microarray. The total number of microarrays is 84. Up denotes the number of upregulated genes. Down denotes the number of downregulated genes

GEO gene expression omnibus, *GDS* GEO datasets

Affymetrix microarrays that investigated both aging and the CR condition in GEO (http://www.ncbi.nlm.nih.gov/geo). Unfortunately, there is no the GDS microarray dataset that tested aging and CR in other tissues such as liver. The DEGs in aging and CR were identified by the criteria of a >2-fold change and a false discovery rate (FDR) <5 using the significance analysis of microarrays program (Tusher et al. 2001). We then combined the DEGs obtained from GDS355, GDS356, GDS2612 (Edwards et al. 2007), and GDS3102 (Linford et al. 2007). GDS355 and GDS356 were tested in the kidney of control-fed 5-month, control-fed 30-month, and calorie-restricted 30-month C57BL/6 mice. GDS2612 was tested in skeletal muscles of control-fed 5-month, control-fed 25-month, and calorie-restricted 25-month C57BL/6NHsd mice (five mice per age group). Detailed information on diet composition and feeding of mouse diets are previously described (Pugh et al. 1999). The CR mice were fed a diet that resulted in a 26 % difference in caloric intake compared to the normal diet animals. GDS3102 was tested in heart and white adipose tissues of control-fed 4-month, control-fed 28-month, and calorie-restricted 28-month Fischer 344 rats (five to seven rats per group). CR (60 % of AL) was initiated at 4 months of age with a switch from the NIH 31 to the NIH-fortified diet. We removed the probes that do not have the gene symbol information for the microarrays and pseudo genes. Also, the DEGs did not contain the genes that have inconsistent fold changes in tissues (nine genes in aging and three genes in CR).

Gene set enrichment analysis

In order to classify genes in the aging and CR transcriptomes, we performed an analysis that assigned to previously defined pathways, genes that significantly differed between aging and young, and aging and CR, in the gene set enrichment analysis (Mootha et al. 2003). The representative terms for biological pathways were used in the context of the Kyoto Encyclopedia of Genes and Genomes (KEGG) (http://www.genome.ad.jp) as suggested by MsigDB v3.0 (http://www.broadinstitute.org/gsea/msigdb). The pathway terminologies mapped to the DEGs in the aging and CR transcriptomes are listed in these databases. Further, we used Fisher's exact *t* test and FDR to map the pathways (Filtering options: $p<10^{-4}$ and FDR<5). The FDR was calculated by qvalue R package (http://www.bioconductor.org/). Because gene set enrichment analysis depends on the gene sets defined as a pathway, we checked various pathway terms using the BioCarta (http://www.biocarta.com) and Reactome (http://www.reactome.org) databases as well as the KEGG database.

Construction of the protein–protein interaction network

In order to construct a PPI network composed of DEGs, we used the Human Protein Reference Database (HPRD) Release 9 (Peri et al. 2003), which was assembled from a combination of experimental PPI information in humans. Although the usage of the human interactome might lead

to false discovery in predicating key molecules among genes in mouse and rat, we used the human interactome because its information has been evaluated by in vivo and in vitro experiments, and the human interactome has much greater information than other species such as mouse and rat. The DEGs were converted to proteins by matching them to official symbols at Entrez (http://www.ncbi.nlm.nih.gov/Entrez/). To visualize the PPI network, we used the Cytoscape program (http://www.cytoscape.org/).

Detection of key molecules with topological metrics

To identify key molecules, we performed a PPI network analysis with topological metrics such as degree and betweenness centrality using the graph module of the Perl program (Newman 2005). Proteins with a high number of interacting partners in the network were regarded as degree-based hubs. Proteins with many short paths between other proteins were regarded as betweenness-based hubs. These topological metrics have been shown to improve the detection of essential genes and are a good method for investigating potential disease genes (Yu et al. 2007; Barabasi et al. 2011). In the PPI network, while we selected the key molecules by the clustering method using degree and "betweenness centrality," we also used clustering analysis with the aim of dividing the group that has a high degree and betweenness centrality along with extra groups because the group with the highest probability might be an essential group of proteins. We performed the clustering analysis using various methods such as hierarchical, K-means, and self-organizing maps algorithms and the validation of the three clustering results using clValid package (http://cran.r-project.org/web/packages/clValid). As a result, the genes were divided into two groups (59 genes upregulated in aging but downregulated by CR) and three groups (60 genes downregulated in aging but upregulated by CR) using hierarchical clustering. In the groups having the highest degree and betweenness centrality, there were three genes (upregulated in aging but downregulated by CR) and two genes (downregulated in aging but upregulated by CR) (Fig. 3b).

Experimental materials

All chemical reagents were purchased from Sigma (St. Louis, MO, USA), except where noted. Damnacanthal, PP2, and L-N5-(1-iminoethyl)ornithine were from Calbiochem (San Diego, CA, USA). Anti-LCK and anti-IκBα antibodies were obtained from Santa Cruz Biotechnology (Santa Cruz, CA, USA), and anti-p-LCK (Tyr 394), anti-p-tyrosine, and anti-p-LCK (Tyr 505) antibodies were from Abnova Corporation (Jhongli City, Taoyuan, Taiwan). The Antibody Beacon™ tyrosine kinase assay kit was obtained from Molecular Probes, Inc. (Eugene, OR, USA). Trizol® was purchased from Invitrogen Co. (Carlsbad, CA, USA). Primers for reverse transcriptase-polymerase chain reaction (RT-PCR) were synthesized by Bioneer, Inc. (Daejeon, Korea). Sterile plasticware for tissue culture were purchased from SPL Labware (Seoul, Korea). All other materials used were of the highest available grade.

Animals

Young (6-month-old) and old (24-month-old) specific pathogen-free (SPF) male Fischer 344 rats and chow were obtained from Samtako (Osan, Korea). Rat maintenance procedures for SPF status and dietary composition of chow have been previously reported (McCarter et al. 1985). Briefly, male SPF Fischer 344 rats were fed a diet of the following composition: 21 % soybean protein, 15 % sucrose, 43.65 % dextrin, 10 % corn oil, 0.15 % α-methionine, 0.2 % choline chloride, 5 % salt mix, 2 % vitamin mix, and 3 % Solka-Floc. The ad libitum (AL)-fed group had free access to both food and water. The animals designated as CR were fed 60 % of the food intake of their AL-fed littermates for 4 weeks. Rats at 6 and 24 months of age were sacrificed by decapitation, and the kidneys were quickly removed and rinsed in ice-cold saline. The tissue was immediately frozen in liquid nitrogen and stored at −80°C. For the histopathological examination of aged kidney in Fischer 344 rats, we followed protocols of Iwasaki et al. (1988) using chow that contained soy protein that eliminated the incidence of glomerulonephritis even at 24 months. In that report, all the pathological analysis was done by two board-certified pathologists (Iwasaki et al. 1988). The animal protocol used in this study was reviewed and approved by the Pusan National University-Institutional Animal Care and Use Committee for its ethical procedures and scientific care.

Tissue preparation for cytosolic extraction

Frozen kidney tissue (200 mg) was homogenized in 1 mL of hypotonic lysis buffer (10 mM HEPES, pH 7.8; 10 mM KCl; 2 mM MgCl2; 1 mM dithiothreitol

(DTT); 0.1 mM EDTA; 0.1 mM PMSF; 1 μM pepstatin; and 2 μM leupeptin) using a tissue homogenizer for 20 s. Homogenates were kept on ice for 20 min, and then 125 μL of 10 % Nonidet P (NP)-40 solution was added and mixed for 15 s. The mixture was centrifuged at 12,000×*g* for 3 min at 4°C, and then supernatants were used as cytosolic protein fraction.

Cell culture and lysis

The Raw 264.7 mouse macrophage cell line was obtained from ATCC (Manassas, VA, USA). The cells were grown in Dulbecco's modified eagle's medium (Nissui, Tokyo, Japan) containing 2 mM L-glutamine, 100 mg/mL penicillin–streptomycin, 2.5 mg/L amphotericin B, and 10 % heat-inactivated fetal bovine serum. Cells were maintained at 37°C in a humidified atmosphere containing 5 % CO_2/95 % air. For cell lysis, cells were rinsed with ice-cold PBS and harvested with a cell scraper followed by centrifugation. The cell pellets were suspended in 10 mM Tris, pH 8.0, with 1.5 mM $MgCl_2$, 1 mM DTT, 0.1 % NP-40, and protease inhibitors, and incubated on ice for 15 min. The cytosolic supernatants were removed by centrifugation at 14,000×*g* at 4°C for 15 min, and the precipitated pellets were suspended in 10 mM Tris, pH 8.0, with 50 mM KCl, 100 mM NaCl, and protease inhibitors, incubated on ice for 30 min, and then they were centrifuged at 14,000×*g* at 4°C for 15 min.

PTK activity

Protein tyrosine kinase activity was assayed in the tissue homogenates and cell lysates using the Antibody Beacon™ tyrosine kinase assay kit (Molecular Probes). To detect tyrosine kinase activity, samples were prepared in 1× kinase buffer (100 mM Tris–HCl, pH 7.5; 20 mM $MgCl_2$; 2 mM EGTA; 2 mM DTT; and 0.02 % Brij 35) and mixed with the Antibody Beacon detection complex plus substrate in a 96-well microplate. ATP reagent was added to the plate and continuously incubated at the reaction temperature. Fluorescence was measured at multiple time points on a GENios (Tecan Instruments, Salzburg, Austria) with excitation and emission wavelengths set at 485 and 535 nm, respectively.

Determination of $ONOO^-$

For the determination of intracellular $ONOO^-$ generation in Raw 264.7 cells, cells were seeded in a 96-well plate. The next day, the cells were exchanged into 10 % fetal bovine serum (FBS) medium containing 60 μM DHR123 and incubated at 37°C for 30 min, and then, the medium was replaced with fresh 10 % FBS containing medium with or without inhibitors for pre-treatment as designated. Then, LPS (*Escherichia coli* O111:B4) at the designated concentration was added to the cells, and the change in fluorescence was immediately measured using a fluorescence plate reader, GENios (Tecan Instruments), at the excitation and emission wavelengths of 485 and 530 nm, respectively.

RT-PCR

For the isolation of total RNA, the kidney sample was homogenized in the presence of TRIzol (2 mL/100 mg of tissue) with a polytron homogenizer (BioSpec Products, Inc., Bartlesville, OK, USA). Chloroform (1/10 volume) was added to the above sample mixture. The samples were shaken vigorously followed by incubation on ice for 5 min. After centrifugation twice at 13,000×*g* for 15 min at 4°C, the supernatant was removed. The RNA pellet was precipitated with isopropanol, washed with 75 % ethanol, dried, and then dissolved in diethyl pyrocarbonate-treated water. cDNA was synthesized using ImProm-II reverse transcriptase (Promega, Madison, WI, USA). PCR was performed using standard protocols. Primers were designed as follows: BlK sense, 5′-TGAAGAGGAGCGTTTTGTGG-3′, anti-sense, 5′-GGGATTTCCCATTCGTCTTG-3′; cSrc sense, 5′-TCGCCCGAAGGAATAGATTT-3′, anti-sense, 5′-AAACCAAAGGTCATGGAGGG-3′; FYN, sense, 5′-TCGATGTAAGCCATTCCTGC-3′, anti-sense, 5′-AGAGCGAAACCACCA AAGGT-3′; HCK, sense, 5′-TTGATGGTGAAGGAGCCAAA-3′, anti-sense, 5′-AGTGGCGGTGAAGACAATGA-3′; LCK, sense, 5′-TTTCACTGCCACC TTCGTGT-3′, anti-sense, 5′-GACTTGGGCTTTGAAAAGGG-3′; LYN, sense, 5′-AGGC TTCTCCATGATTGCCT-3′, anti-sense, 5′-CCCCCAGAAAATGAGACGAT-3′. ß-Actin was used as an internal control.

Immunoprecipitation

The cell lysates were subjected to immunoprecipitation in a buffer containing 40 mM Tris, pH 7.6; 120 mM NaCl; 5 mM EDTA; 0.1 % NP40; 0.25 %

deoxycholic acid; protease inhibitors; and phosphatase inhibitors. A sample (1 mg) was incubated with a 50 % slurry of protein A at 4°C for 2 h for pre-cleaning. After incubation, the sample was centrifuged at 12,000×*g* for 10 min at 4°C. Samples were incubated with respective antibodies at 4°C overnight, followed by incubation with a 50 % slurry of protein A agarose at 4°C for 3 h. After washing with the IP buffer, the immunoprecipitated proteins were analyzed by Western blotting.

Western blotting

Homogenized samples were boiled for 5 min in a gel-loading buffer (0.125 M Tris–HCl, pH 6.8; 4 % sodium dodecyl sulfate (SDS); 10 % 2-mercaptoethanol; and 0.2 % bromophenol blue) at a ratio of 1:1. An equal total protein amount for each sample was separated by SDS-polyacrylamide gel electrophoresis using 10 % acrylamide gels, and the bands were transferred to a PVDF membrane. The membrane was blocked at room temperature for 1 h and was incubated with specific primary antibody at 25°C for 4 h, followed by a horseradish peroxidase-conjugated secondary antibody at 25°C for 1 h. Antibodies were detected using West-zol Plus (iNtRon Biotechnology, Seongnam, Korea) and chemiluminescence FluorchemTMSP (Alpha Innotech Corporation, San Leandro, CA, USA).

Statistical analysis for experimental results

The results are expressed as the mean±SE from triplicate assays with five separate experiments. The statistical significance of the differences between groups was determined by single-factor ANOVA followed by Fisher's protected LSD post hoc test. The p values <0.05 were considered statistically significant.

Results

Differentially expressed genes in aging and the CR paradigm

We selected four microarray datasets from investigations of both aging and CR. The microarray data were designed to model young versus old (representing aging) and old versus CR (representing calorie restriction) in mouse and rat. As a result, we obtained 1,075 DEGs, which we collectively termed the aging and CR transcriptome; 740 genes were expressed differentially in aging, whereas 565 genes were expressed differentially in CR (Fig. 1). A total of 230 genes were changed significantly in both aging and the CR condition; 103 genes were upregulated in aging but downregulated by CR, and 121 genes were downregulated in aging but were upregulated by CR. The differentially expressed genes in aging and CR overlapped (31 and 41 % of the age- and CR-related DEGs, respectively). Detailed information about the DEGs in aging and the CR condition is provided in Table S1. Among the DEGs, there were several notable genes known to be associated with pathways that are aging related, such as the immune response, inflammation, energy metabolism, and insulin signaling. The genes upregulated by aging included genes that encode the nuclear factor of kappa light polypeptide gene enhancer in B cell inhibitor, alpha (NF-κB1α), which is known as the transcription factor for pro-

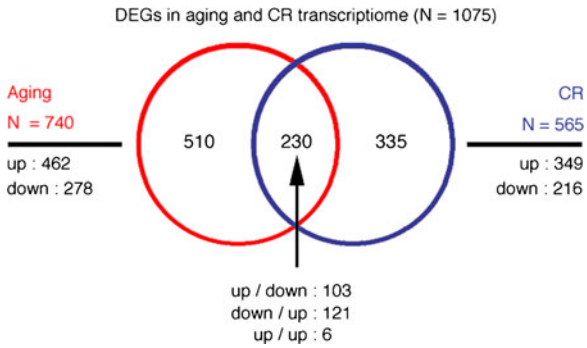

Fig. 1 Comparison of differentially expressed genes in the aging and CR transcriptomes. The *red circle* (aging) represents genes differentially expressed between young and old. The *blue circle* (CR) represents genes differentially expressed between old and CR. The microarrays used were 84 cDNA microarrays from GEO (GDS355, GDS356, GDS2612, and GDS3102). The dataset was tested on kidney, skeletal muscle, heart, and white adipose tissues in mouse and rat, and the all microarray experiments were designed as models of young versus old and old versus CR. The DEGs were identified by the criteria of a >2-fold change and a false discovery rate <5. As a result, we obtained 1,075 DEGs, which we collectively termed the aging and CR transcriptome; 740 genes were expressed differentially in aging, whereas 565 genes were expressed differentially in CR. A total of 230 genes were changed significantly in both aging and the CR condition; 103 genes were upregulated in aging but downregulated by CR, and 121 genes were downregulated in aging but were upregulated by CR. The differentially expressed genes in aging and CR overlapped (31 and 41 % of the age- and CR-related DEGs, respectively)

inflammatory genes; tumor necrosis factor receptor superfamily, known as the receptor for a key pro-inflammatory cytokine; and 90-kDa ribosomal protein S6 kinase, polypeptide 3 (RPS6KA3), which is related to mTOR. In addition, the genes downregulated by CR included the insulin-like growth factor binding protein 3, which is closely related to insulin growth factor, and cathepsin S (CTSS), which is known as a harbinger of an increased risk of death among elderly people (Jobs et al. 2011).

Gene set enrichment analysis of the aging and CR transcriptomes

In the aging transcriptome, 14 pathways were represented by upregulated genes using the KEGG terminologies (Fig. 2a and Table S2). Genes related to the immune response and inflammation were mostly upregulated with aging, such as "cytokine–cytokine receptor interaction" ($p=2.52\times10^{-11}$), "natural killer cell-mediated cytotoxicity" ($p=3.41\times10^{-11}$), and "primary immunodeficiency" ($p=1.92\times10^{-9}$). The activation of genes involved in inflammation is considered a possible underlying basis for the molecular alterations in aging and age-related diseases. In addition, activation of the "complement and coagulation cascades" ($p=3.30\times10^{-11}$) is known as the major cause of age-related macular degeneration with chronic inflammation (Anderson et al. 2010), and "cell adhesion molecules cams" ($p=3.92\times10^{-5}$) reportedly increases during aging; these increases were blocked by CR (Zou et al. 2004). In contrast, 14 pathways were represented by the downregulated genes in the aging transcriptome (Fig. 2a and Table S2). Genes employed in energy metabolism showed a marked trend toward downregulation, such as "pyruvate metabolism" ($p=2.22\times10^{-12}$), "steroid biosynthesis" ($p=8.66\times10^{-11}$), "glycolysis gluconeogenesis" ($p=5.03\times10^{-9}$), and "citrate cycle TCA cycle" ($p=9.94\times10^{-6}$).

In the CR transcriptome, four pathways were represented by the upregulated genes (Fig. 2b and Table S2). The pathways were largely related to energy metabolism, such as pyruvate metabolism ($p=6.02\times10^{-10}$), glycolysis gluconeogenesis ($p=5.31\times10^{-7}$), citrate cycle TCA cycle ($p=2.96\times10^{-5}$), and steroid biosynthesis ($p=3.55\times10^{-5}$). Genes regulating the immune response, such as those involved in primary immunodeficiency ($p=1.60\times10^{-7}$) and natural killer cell-mediated cytotoxicity ($p=5.69\times10^{-5}$), were downregulated in CR; however, these genes were upregulated in aging. These observations are consistent with a previous report (Lee et al. 2002). In addition, the genes involved in energy metabolism were mostly upregulated in CR and downregulated in aging. According to BioCarta and Reactome terminologies, most genes employed in energy metabolism were decreased, in contrast to most immune response and inflammation-related genes, which were increased (Table S2).

Genes shared between aging and CR

To determine the relation between aging and CR, DEGs in both biological processes were first identified, and then the shared characteristics of the aging and CR DEGs were investigated using the strategy described in the previous section. A total of 230 genes were differentially expressed in both processes; 103 genes were upregulated in aging but were downregulated by CR, 121 genes were downregulated in aging but were upregulated by CR, and six genes were upregulated in aging and were upregulated by CR. The differentially expressed genes in aging and CR overlapped and included 31 and 41 % of the age- and CR-related DEGs, respectively. The up- or downregulated profiles of the gene sets are described in Fig. 2c. The genes governing primary immunodeficiency ($p=1.91\times10^{-9}$), natural killer cell-mediated cytotoxicity ($p=4.34\times10^{-7}$), and hematopoietic cell lineage ($p=1.24\times10^{-5}$) biased the distribution of upregulation in aging and downregulation in CR. The genes involved in pyruvate metabolism ($p=4.42\times10^{-14}$), glycolysis gluconeogenesis ($p=1.36\times10^{-10}$), citrate cycle TCA cycle ($p=1.66\times10^{-7}$), steroid biosynthesis ($p=5.73\times10^{-7}$), and PPAR signaling pathway ($p=8.25\times10^{-6}$) biased the distribution of downregulation in aging and upregulation in CR (Fig. 2c).

Prediction of key molecules based on the PPI network

From gene set analysis, we discovered important pathways in gaining a better understanding of the biological relationship between aging and CR. More interestingly, some genes that were identified in both transcriptomes were regulated in an opposite manner by aging and CR. However, because many differentially expressed genes were dropped, it is difficult to select important key molecules that regulate aging,

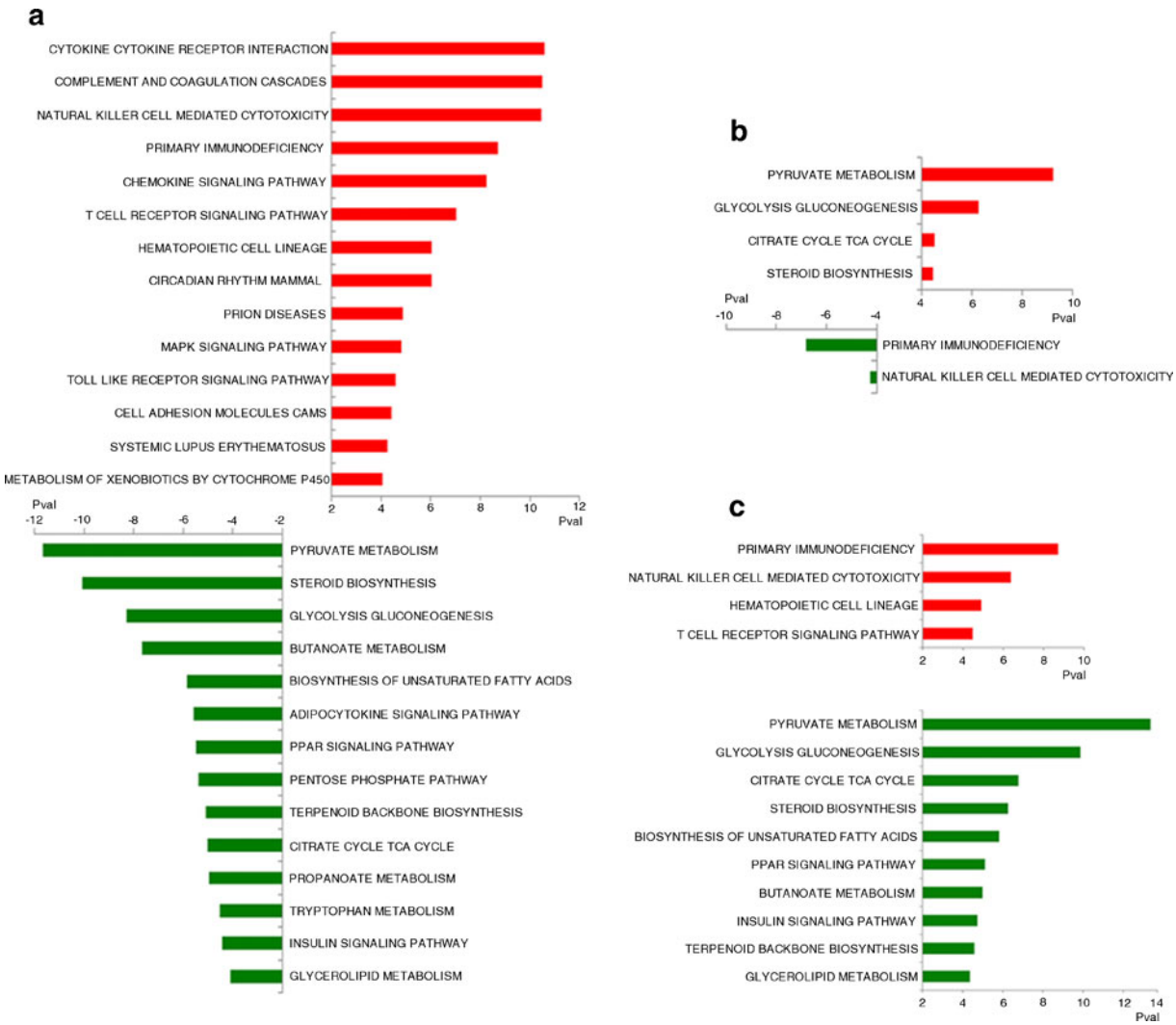

Fig. 2 Gene sets enriched in the aging and CR transcriptomes. Classification of the aging and CR transcriptomes in the context of KEGG terminologies. The mapping terminologies (pathways) were selected by Fisher's exact *t* test and false discovery rate (filtering options: $p<10^{-4}$ and FDR<5). *Red bars* indicate upregulated gene sets and *green bars* represent downregulated gene sets in each condition. *Pval* means the modified significant value that is calculated by the following equation: ± [−log(*p* value)]. + means upregulated gene set, and − means downregulated gene set. **a** Distribution of the aging transcriptome with respect to biological process. **b** Distribution of the CR transcriptome with respect to biological process. **c** Distribution of genes shared in both the aging and CR transcriptomes

such as those seen in the CR effect. Therefore, we performed a PPI network analysis that has been previously applied to identify essential molecules, such as a hub, because the PPI network has been successfully applied to discover essential genes, disease genes, and drug targets in yeast to human (Jeong et al. 2001; Taylor et al. 2009).

To identify the key molecules, the genes were converted to proteins using official symbols. We then constructed a PPI network composed of 119 genes (59 genes upregulated in aging but downregulated by CR and 60 genes downregulated in aging but upregulated by CR) among 230 genes, which is shown in Fig. 3a. We attempted a protein–protein interaction of all 230 genes. However, only 119 genes reported protein–protein interaction information in the HPRD. No information is available on the protein–protein interaction of 111 genes. From the PPI network analysis, we chose three genes among the genes that are upregulated in aging but downregulated by CR and

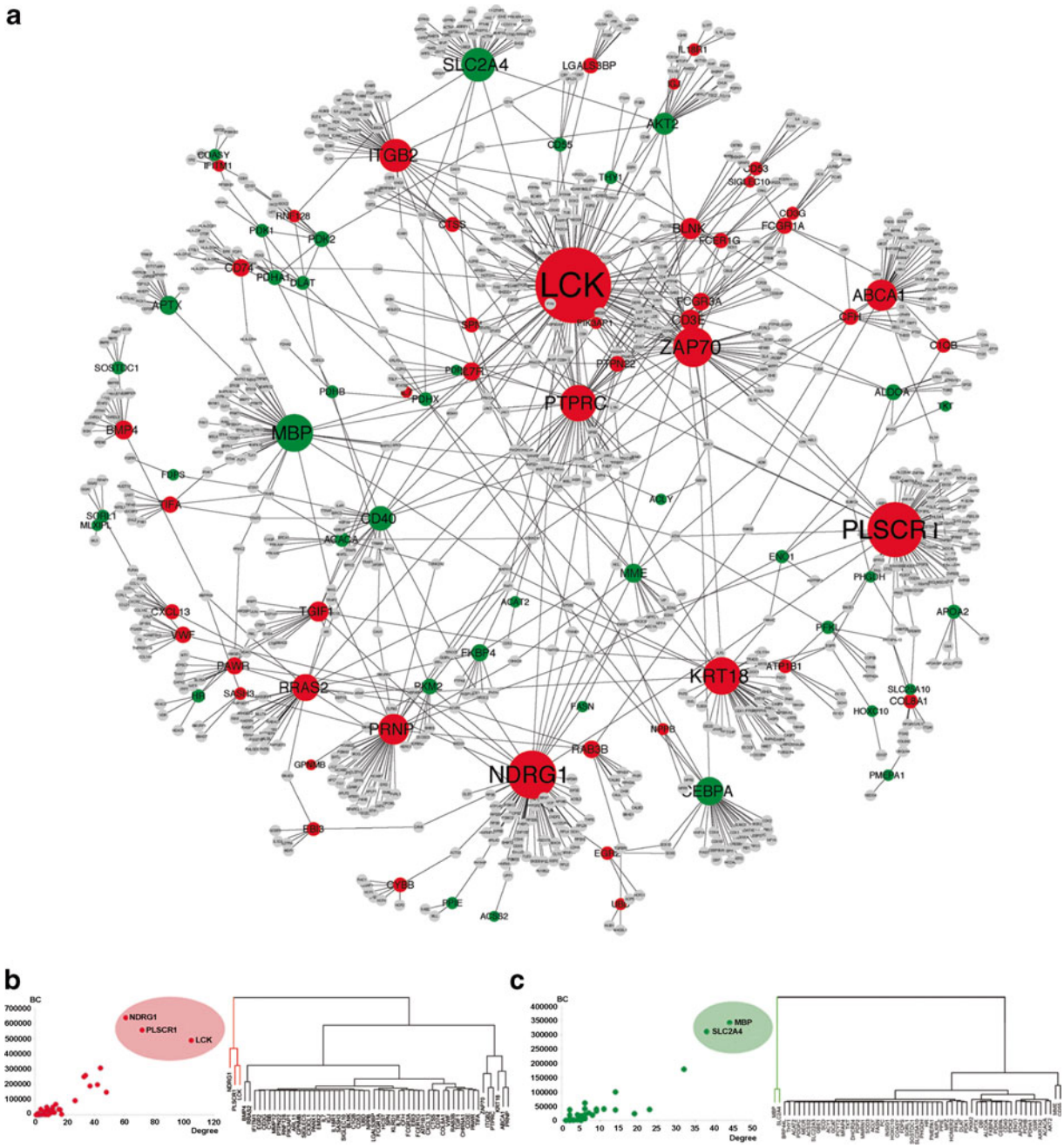

Fig. 3 Protein–protein interaction network composed of common differentially expressed genes in both aging and CR. **a** The PPI network, in which the nodes represent proteins, and the edges represent the interactions between the proteins inferred from the HPRD database. The network consisted of 119 proteins and 1,156 interactions. A total of 59 proteins that were upregulated in aging but downregulated by CR are represented in *red*, and 60 proteins that were downregulated in aging but upregulated by CR are represented in *green*. The node sizes correlate with the number of interacting partners (degrees). *Gray colors* are the proteins that were obtained from the HPRD database and interacted with the DEGs. **b** The distribution and hierarchical clustering of degree and betweenness centrality for proteins upregulated by aging but downregulated by CR. **c** The distribution and hierarchical clustering of degree and betweenness centrality for proteins downregulated by aging but upregulated by CR. We used clustering analysis, with the aim of dividing the group that has high degree and betweenness centrality and extra groups. From this clustering result, we chose LCK, PLSCR1, and NDRG1 from the DEGs that are upregulated in aging but downregulated by CR, and MBP and SLC2A4 (GLUT4) from the genes that are downregulated in aging but upregulated by CR

two genes among the genes that are downregulated in aging but upregulated by CR. The list of key molecules and network properties is described in Table 2.

As a result, we found that LCK, phospholipid scramblase 1 (PLSCR1), and NMYC downstream regulated gene 1 (NDRG1) are predicted as key molecules having higher degree and betweenness centrality scores than the other proteins in the PPI network (Fig. 2b). LCK is well known as a T cell receptor-associated protein tyrosine kinase. Specifically, oxidative stress leads to the activation and expression of LCK (Hardwick and Sefton 1995). LSCR1 is a lipid-binding protein that enters the nucleus and promotes the recruitment and activation of Src kinases (Dong et al. 2004). Specifically, PLSCR1 is critical to the normal regulation of fat accumulation in mice, and abdominal fat accumulation with the formation of enlarged lipid-engorged adipocytes has emerged as the key risk factor for the onset of type 2 diabetes (Greenberg and McDaniel 2002). NDRG1 is a member of the N-myc downregulated gene family, which belongs to the alpha/beta hydrolase superfamily. Upregulation of NDRG1 has been observed in both old age and in Werner's syndrome (Kyng et al. 2003).

In contrast, myelin basic protein (MBP) and glucose transporter (SLC2A4) were selected as key molecules among the aging downregulated and CR upregulated genes. MBP, a major constituent of the myelin sheath of oligodendrocytes, is reported to decrease in aging. Furthermore, age-related loss of myelin is correlated with a decline in nerve strength, and CR interventions, which slow myelin loss, also preserve functional nerve performance (Rangaraju et al. 2009; Ingram et al. 2007). SLC2A4, which is also known as GLUT4, is involved in insulin signaling and insulin resistance. Therefore, upregulation of SLC2A4 leads to insulin sensitivity, which supports the fact that CR improves insulin sensitivity. Some reports have stated that GLUT4 is induced by CR and regulates energy metabolism in white adipose tissue (Park et al. 2008).

Effects of aging and CR on SFK levels and LCK activity

We selected a candidate gene for experimental evaluation among the genes that were upregulated in aging but downregulated by CR, because these genes act like a CR mimic, that is, as an aging modulator. Among three candidate genes, we chose LCK, which had the highest score of degree in the PPI network (Fig. 3a). We then confirmed the changes in the expression and activity of LCK in aged rat kidney. The kidney is among the most studied organs for aging and calorie restriction, making for more published data available in the literature. In addition, the kidney is most responsive to the anti-aging effects of calorie restriction according to many previous reports including our own studies.

There are in fact several Src families of tyrosine kinases (SFKs), including LCK, HCK, LYN, and Src (Martin 2001). Therefore, we attempted to verify the differences in the expression of other SFKs in addition to LCK in the rat kidney during aging and under CR conditions. To determine changes of the gene expression of nine types of SFKs during aging, an RT-PCR assay was performed to measure the abundance of SFK mRNAs in young and old AL and CR rats. As shown in Fig. 4a, among the SFK mRNAs, we only

Table 2 Key molecules predicted by the PPI network composed of DEGs

Symbol	Description	Degree	BC*
Upregulated by aging but downregulated by CR			
LCK	Lymphocyte-specific protein tyrosine kinase	105	490,166
PLSCR1	Phospholipid scramblase 1	72	558,469
NDRG1	NMYC downstream regulated gene 1	61	639,109
Downregulated by aging but upregulated by CR			
MBP	Myelin basic protein	44	343,376
SLC2A4	Solute carrier family 2 member 4	38	312,131

Degree refers to the number of interacting partners in the protein–protein interaction network. BC refers to the scores of betweenness centrality in the protein–protein interaction network

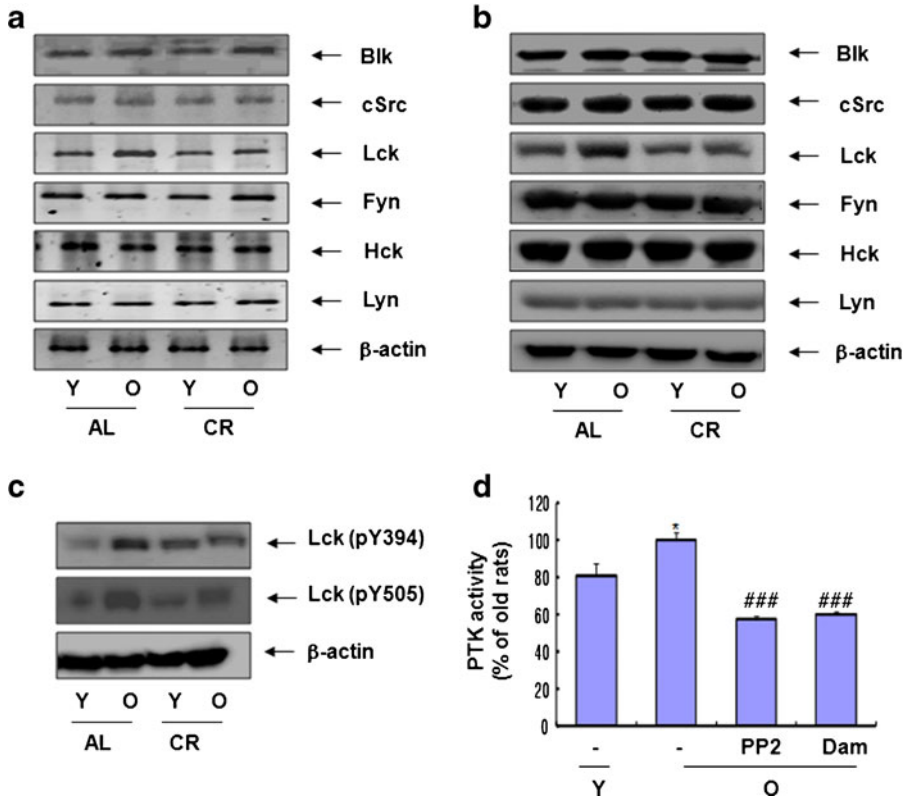

Fig. 4 Changes in the mRNA levels, protein levels, and activity of LCK, and the effect of SFKs and LCK on PTK activity upregulation during aging. **a** RT-PCR analysis of BLK, cSrc, LCK, FYN, HCK, and LYN was performed using RNA isolated from young (*Y*) and old (*O*) AL and CR rats. ß-Actin primers were used in separate PCR reactions to control for the efficiency of cDNA synthesis in each sample. **b** and **c** Western blotting was performed to detect total LCK protein levels and the tyrosine phosphorylation status (p394 and p505) of LCK from AL and CR rats. ß-Actin was used as a loading control for the cytosolic and membrane fraction samples. One representative blot is shown from three independent experiments that yielded similar results. **d** PTK activity was measured in kidney homogenates from Y and O rats. PTK activity was measured in the presence or absence of tyrosine kinase inhibitor, Src kinase inhibitor (PP2, 5 μM), or LCK inhibitor [damnacanthal (Dam), 40 nM]. Each value is the mean±SE of five rats. The results of one-factor ANOVA: $*p<0.05$ vs. young rats; $###p<0.001$ vs. age-matched old rats

observed an apparent increase in LCK levels. Compared with young AL rats, old AL rats had increased LCK mRNA levels, whereas old CR rats had lower levels of LCK than their AL counterparts. Three types of mRNAs (Fgr, Yes, and Yrk) did not appear in the aged kidney.

Based on the results of the mRNA level measurements, we next investigated the changes in LCK protein levels and activity by Western blotting using both an anti-total LCK- and an anti-p-LCK (Tyr 394 or 505)-specific antibody in kidney homogenates. The results, shown in Fig. 4b and c, demonstrated that both the protein and activity levels of LCK increased with age in AL rats, while CR inhibited this change.

To better understand the involvement of SFKs and LCK in PTK activity during aging, we measured PTK activity in kidney homogenates in the presence or absence of SFK inhibitor (PP2) and LCK inhibitor (damnacanthal). The results showed that PTK activity increased in old rats compared with young rats and that this age-related upregulation was decreased in the presence of PP2 (approximately 50 %) or damnacanthal (approximately 40 %) (Fig. 4d). Therefore, these results indicate that SFKs participate in the remarkably increased PTK activity observed during aging and that among the SFKs, LCK in particular, may play an important role in the regulation of PTK activity in the aged kidney.

Involvement of LCK in the NF-κB signaling pathway through LPS-induced $ONOO^-$ generation

In a previous study, LCK was shown to mediate crystalline silica-induced NF-κB activation through

tyrosine phosphorylation of IκBα in Raw 264.7 cells (Kang et al. 2006). On the basis of the result shown in Fig. 4, we sought to elucidate the LCK-induced activation of the NF-κB signaling pathway in LPS-treated Raw 264.7 cells. SFKs are known to be activated by autophosphorylation at tyrosine residues in response to ROS (Giannoni et al. 2010). To investigate whether redox-sensitive LCK is activated by LPS treatment, we initially looked for intracellular $ONOO^-$ generation. The results show that intracellular $ONOO^-$ was unchanged at early times, but increased from 6 h and reached maximal levels at 12 h after the LPS treatment (Fig. 5a). However, the addition of penicillamine (an $ONOO^-$ inhibitor) and L-N5-(1-iminoethyl)-ornithine

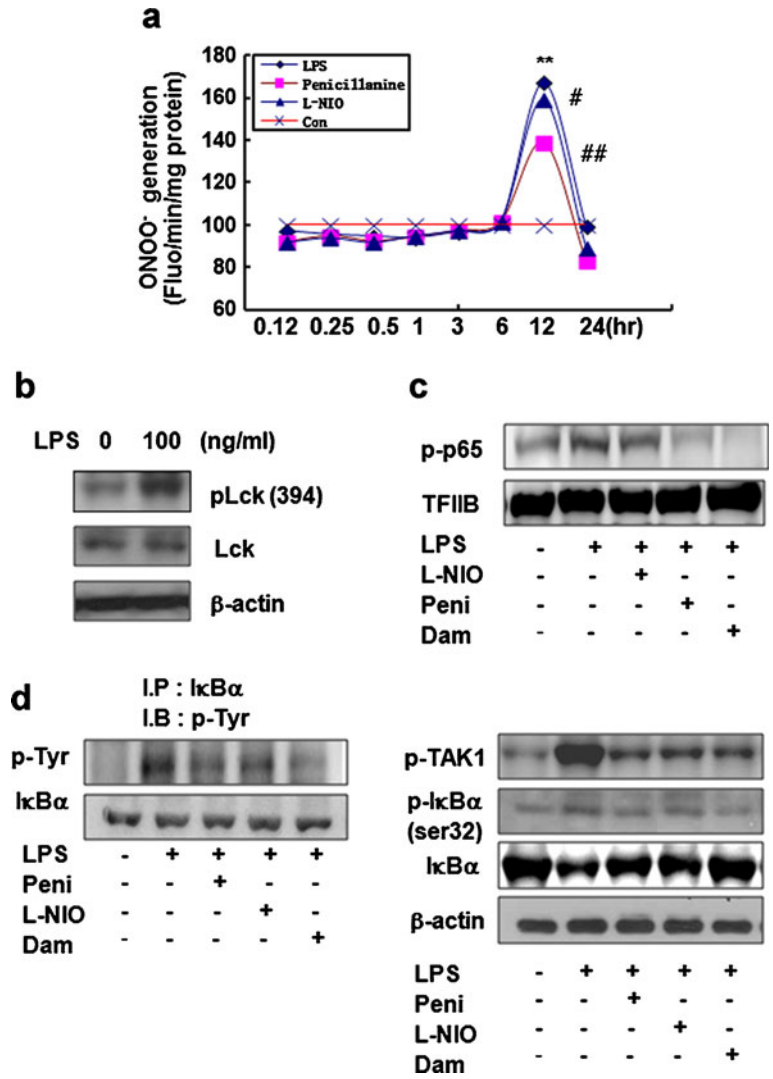

Fig. 5 NF-κB activation by LCK induction in Raw 264.7 cells stimulated with LPS. **a** LPS (100 ng/mL)-induced accumulation of intracellular $ONOO^-$ was monitored by DHR123. The time course of changes in fluorescence was monitored with a GENios Plus fluorescent microplate reader. **b** Raw 264.7 cells were exposed to LPS (100 ng/mL) for 12 h. The levels of anti-LCK and anti-p LCK antibody were detected by Western blotting. ß-Actin was used as a loading control. **c** Raw 264.7 cells were pre-incubated for 2 h with L-NIO (100 μM), penicillamine (100 μM), or damnacanthal (170 nM) before treatment with LPS (100 ng/mL) for 12 h. The level of p-p65 NF-κB was detected in the nucleus by Western blotting. TFIIB was used as a loading control. **d** (*left*) Cell lysates were immunoprecipitated with anti-IκBα antibody followed by Western blotting with anti-p-tyrosine antibody. **d** (*right*) Cell lysates were analyzed by Western blotting with anti-p-TAK1 or anti-p-IκBα (serine 32) antibody. ß-Actin was used as a loading control. One representative blot is shown from three independent experiments that yielded similar results

(L-NIO) (a NOS inhibitor) prevented this change. LCK was also activated 12 h after LPS treatment (Fig. 5b). Therefore, the results shown in Fig. 5a and b suggest that LCK is activated by LPS-induced $ONOO^-$ generation in Raw 264.7 cells.

Next, to determine whether LCK induction by $ONOO^-$ leads to NF-κB activation through tyrosine phosphorylation by IκBα, we examined the phosphorylation status of NF-κB and IκBα after LPS treatment in the presence or absence of an $ONOO^-$ inhibitor (penicillamine), a NOS inhibitor (L-NIO), and an LCK inhibitor (damnacanthal). As shown in Fig. 5c, LPS stimulation induced significant serine phosphorylation of p65, which was substantially decreased in the presence of $ONOO^-$ inhibitor, LCK inhibitor, or NOS inhibitor. These results suggest that LPS-triggered NF-κB activation was caused by the activation of LCK through $ONOO^-$ generation. Then, to determine whether LCK activates NF-κB through tyrosine phosphorylation of IκBα, LPS-treated cell lysates were immunoprecipitated with an anti- IκBα antibody followed by immunoblotting with anti-phosphotyrosine antibody. The results showed that tyrosine phosphorylation of IκBα was observed 12 h after LPS stimulation, and this phosphorylation was decreased by treatment with all three inhibitors (Fig. 5d). Therefore, these data suggest that LCK participates in the tyrosine phosphorylation of IκBα, leading to NF-κB activation through LPS stimulation. Interestingly, we showed that LCK triggers serine phosphorylation of IκBα and its upstream serine kinase TAK1, as well as the subsequent degradation of IκBα (Fig. 5d). Therefore, we suggest that LCK causes NF-κB activation through serine or tyrosine phosphorylation of IκBα in an $ONOO^-$ generation-dependent manner.

Discussion

Although the major mechanisms underlying the aging process and its modulation are not fully understood, CR has been intensely studied for its intervening effect on the aging process. Some gerontologists have proposed that CR might provide protection from the common diseases of aging (Weindruch et al. 2001). Many studies have reported that the proximal causes of aging and longevity regulators are both closely connected to CR, and both are essential to understanding what underlies the aging process (Yu et al. 2005; Chung et al. 2002).

In our study, we determined that the immune response and energy metabolism mainly differed in the cDNA microarrays on aging and CR as shown in Fig. 2c. Aging leads to the upregulation of the immune response but the downregulation of genes related to metabolism and biosynthesis. However, CR leads to downregulation of the immune response but upregulation of energy metabolism and biosynthesis. These results are consistent with the current understanding of the dichotomous relationship between aging and CR. For instance, in the aging process, the upregulation of immune response is closely related to inflammation and ROS production in the cell. Also, the downregulation of energy metabolism is indicative of the reduction in the mitochondrial respiratory rate and gluconeogenic capacity. These downregulated pathways are closely involved in the degeneration of the human body because muscle and other tissues utilize amino acids derived from protein turnover to generate energy via the TCA cycle (Goodman et al. 1980). On the other hand, energy metabolism and biosynthesis-related pathways promote the activity of cells by CR. These findings suggest that CR could reduce ROS production by downregulating the immune response and could reduce the level and accumulation of damaged proteins throughout the body by enhancing the turnover and replacement of proteins in old age by upregulating energy metabolism pathways.

Our analyses revealed further important insights: the immune response and energy metabolism-related genes that modulate aging-related biological processes may be oppositely regulated by CR. The immune response is already a well-known pathway that is upregulated in aging but downregulated by CR, because the immune response is a major source of oxidative stress in the cell. In addition, several papers have reported that CR promotes the turnover and replacement of proteins in old age (Goto et al. 2002; Dhahbi et al. 2005). Enhanced turnover should reduce the dwell time of proteins and thereby reduce the level and accumulation of damaged proteins throughout the body (Spindler et al. 2003). These findings also support our results that metabolism-related pathways are induced by CR. Additionally, the PPAR signaling pathway is a well-known pathway that is upregulated by CR. Upregulation of the PPAR signaling pathway causes the reduction of fatty acids through beta-

oxidation in ribosomes. Our laboratory reported that PPAR attenuates aging by reducing oxidative stress (Sung et al. 2004).

Based on the biological background, we performed a PPI network analysis to identify key molecules among the differentially expressed genes that are common to both aging and CR. As a result, LCK, PLSCR1, and NDRG1 had high values of degree and betweenness centrality among those genes upregulated in aging but downregulated by CR. In contrast, MBP and SLC2A4 were selected among those genes downregulated in aging but upregulated by CR. We tested LCK as a key molecule for the modulation of aging in mammals because its function is closely related to the immune response and it has the highest degree score among the candidates in the PPI network.

LCK, a member of the Src family non-receptor protein tyrosine kinase, is mostly expressed in T cells and some B cells. Recruitment of LCK to the cell membrane by CD4 and CD8 plays an essential role in T cell activation and development (Artyomov et al. 2010). The lack of LCK expression through development of the homozygous mutant mice severely disrupts thymocyte development (Molina et al. 1992). Also, circulating T cells from the LCK homozygous mice have a significantly decreased proliferative response, calcium mobilization, and IL-2 production (Straus and Weiss 1992; Trobridge and Levin 2001). However, the lack of LCK expression in peripheral mature T cells has no effect on the number of mature circulating T cells or survival of these cells (Seddon et al. 2000). Specially, the $LCK^{-/\pm}$ mutant mice appear healthy; lymphoid organs and thymocyte as well as peripheral T cell populations are normal.

Moreover, previous reports suggest that LCK acts as a proto-oncogene. The overexpression of wild type LCK reproducibly developed thymic tumors, indicating that LCK contributes to the pathogenesis of human neoplastic disease (Abraham et al. 1991). Kamens et al. reported that selective inhibitors of LCK have the potential to be efficacious in preventing T cell-driven inflammatory disease, including rheumatoid arthritis, multiple sclerosis, inflammatory bowel diseases, type I diabetes, systemic lupus erythematosus, and psoriasis (Kamens et al. 2001).

Because T cells often infiltrate into tissues with disease or the aging process (Stichel and Luebbert 2007; Zhang et al. 2003), it explains why the expression and activation of LCK in aged kidney increase immune response and inflammatory factors. Hence, we confirmed that LCK expression was upregulated in aging but downregulated by CR both in vitro and in vivo using kidney obtained from aged and CR rats. Additionally, we performed mRNA expression experiments for four other predicted key molecules (PLSCR1, NDRG1, MBP, and SLC2A4) in aged kidney and under calorie restriction conditions using RT-PCR. The mRNA levels of these four genes were consistent with our bioinformatics prediction (data not shown).

Our major significant findings are that the expression and activity of LCK was modulated by CR in aged rat kidney and that the age-related increase in PTK activity was decreased by a specific inhibitor of LCK. Additionally, we confirmed that induction of LCK by $ONOO^-$ leads to activation of NF-κB through serine or tyrosine phosphorylation of IκBα and that it is modulated by CR. Therefore, these results indicate that LCK could be considered a target protein that is attenuated by the anti-aging effects of CR. In summary, our approaches aim to identify candidate genes that are similar to the CR effect as well as to understand the biological pathway related to aging and the molecular behavior of CR, ultimately to prevent aging in a top–down manner using the integration of cDNA microarray data and the PPI network. Our findings revealed that the immune response and inflammation-related pathways are upregulated in aging, while CR reversed these effects. Energy metabolism and biosynthesis-related pathways were downregulated in aging and were blunted by CR. The present study also suggested key molecules in the PPI networks of aging and CR. In addition, our experimental validation of LCK verifies that this system's biological approach might be a very powerful tool for identifying target proteins for aging intervention as well as a roadmap for aging studies.

Acknowledgments We thank Jungsul Lee for advice on statistical analyses. This work was supported by a National Research Foundation of Korea (NRF) grant funded by the Korean government (MOST) (no. 20090083538). We thank the Aging Tissue Bank for providing research information.

References

Abraham KM, Levin SD, Marth JD, Forbush KA, Perlmutter RM (1991) Thymic tumorigenesis induced by overexpression of p56lck. Proc Natl Acad Sci U S A 88(9):3977–3981

Anderson DH, Radeke MJ, Gallo NB, Chapin EA, Johnson PT, Curletti CR, Hancox LS, Hu J, Ebright JN, Malek G, Hauser MA, Rickman CB, Bok D, Hageman GS, Johnson LV (2010) The pivotal role of the complement system in aging and age-related macular degeneration: hypothesis revisited. Prog Retin Eye Res 29(2):95–112. doi:10.1016/j.preteyeres.2009.11.003

Artyomov MN, Lis M, Devadas S, Davis MM, Chakraborty AK (2010) CD4 and CD8 binding to MHC molecules primarily acts to enhance Lck delivery. Proc Natl Acad Sci U S A 107(39):16916–16921. doi:10.1073/pnas.1010568107

Barabasi AL, Gulbahce N, Loscalzo J (2011) Network medicine: a network-based approach to human disease. Nat Rev Genet 12(1):56–68. doi:10.1038/nrg2918

Chung HY, Kim HJ, Kim KW, Choi JS, Yu BP (2002) Molecular inflammation hypothesis of aging based on the anti-aging mechanism of calorie restriction. Microsc Res Tech 59(4):264–272. doi:10.1002/jemt.10203

Dhahbi JM, Mote PL, Fahy GM, Spindler SR (2005) Identification of potential caloric restriction mimetics by microarray profiling. Physiol Genomics 23(3):343–350. doi:10.1152/physiolgenomics.00069.2005

Dong B, Zhou Q, Zhao J, Zhou A, Harty RN, Bose S, Banerjee A, Slee R, Guenther J, Williams BR, Wiedmer T, Sims PJ, Silverman RH (2004) Phospholipid scramblase 1 potentiates the antiviral activity of interferon. J Virol 78(17):8983–8993. doi:10.1128/JVI.78.17.8983-8993.200478/17/8983

Edwards MG, Anderson RM, Yuan M, Kendziorski CM, Weindruch R, Prolla TA (2007) Gene expression profiling of aging reveals activation of a p53-mediated transcriptional program. BMC Genomics 8:80. doi:10.1186/1471-2164-8-80

Giannoni E, Taddei ML, Chiarugi P (2010) Src redox regulation: again in the front line. Free Radic Biol Med 49(4):516–527. doi:10.1016/j.freeradbiomed.2010.04.025

Goodman MN, Larsen PR, Kaplan MM, Aoki TT, Young VR, Ruderman NB (1980) Starvation in the rat. II. Effect of age and obesity on protein sparing and fuel metabolism. Am J Physiol 239(4):E277–E286

Goto S, Takahashi R, Araki S, Nakamoto H (2002) Dietary restriction initiated in late adulthood can reverse age-related alterations of protein and protein metabolism. Ann N Y Acad Sci 959:50–56

Greenberg AS, McDaniel ML (2002) Identifying the links between obesity, insulin resistance and beta-cell function: potential role of adipocyte-derived cytokines in the pathogenesis of type 2 diabetes. Eur J Clin Invest 32(Suppl 3):24–34

Hardwick JS, Sefton BM (1995) Activation of the Lck tyrosine protein kinase by hydrogen peroxide requires the phosphorylation of Tyr-394. Proc Natl Acad Sci U S A 92(10):4527–4531

Hong SE, Heo HS, Kim DH, Kim MS, Kim CH, Lee J, Yoo MA, Yu BP, Leeuwenburgh C, Chung HY (2010) Revealing system-level correlations between aging and calorie restriction using a mouse transcriptome. Age (Dordr) 32(1):15–30. doi:10.1007/s11357-009-9106-3

Ingram DK, Young J, Mattison JA (2007) Calorie restriction in nonhuman primates: assessing effects on brain and behavioral aging. Neuroscience 145(4):1359–1364. doi:10.1016/j.neuroscience.2006.10.031

Iwasaki K, Gleiser CA, Masoro EJ, McMahan CA, Seo EJ, Yu BP (1988) The influence of dietary protein source on longevity and age-related disease processes of Fischer rats. J Gerontol 43(1):B5–B12

Jeong H, Mason SP, Barabasi AL, Oltvai ZN (2001) Lethality and centrality in protein networks. Nature 411(6833):41–42. doi:10.1038/3507513835075138

Jobs E, Ingelsson E, Riserus U, Nerpin E, Jobs M, Sundstrom J, Basu S, Larsson A, Lind L, Arnlov J (2011) Association between serum cathepsin S and mortality in older adults. JAMA 306(10):1113–1121. doi:10.1001/jama.2011.1246

Kamens JS, Ratnofsky SE, Hirst GC (2001) Lck inhibitors as a therapeutic approach to autoimmune disease and transplant rejection. Curr Opin Investig Drugs 2(9):1213–1219

Kang JL, Jung HJ, Lee K, Kim HR (2006) Src tyrosine kinases mediate crystalline silica-induced NF-kappaB activation through tyrosine phosphorylation of IkappaB-alpha and p65 NF-kappaB in RAW 264.7 macrophages. Toxicol Sci 90(2):470–477. doi:10.1093/toxsci/kfj096

Kirkwood TB (2005) Understanding the odd science of aging. Cell 120(4):437–447. doi:10.1016/j.cell.2005.01.027

Kyng KJ, May A, Kolvraa S, Bohr VA (2003) Gene expression profiling in Werner syndrome closely resembles that of normal aging. Proc Natl Acad Sci U S A 100(21):12259–12264. doi:10.1073/pnas.2130723100 2130723100

Lee CK, Allison DB, Brand J, Weindruch R, Prolla TA (2002) Transcriptional profiles associated with aging and middle age-onset caloric restriction in mouse hearts. Proc Natl Acad Sci U S A 99(23):14988–14993. doi:10.1073/pnas.232308999232308999

Linford NJ, Beyer RP, Gollahon K, Krajcik RA, Malloy VL, Demas V, Burmer GC, Rabinovitch PS (2007) Transcriptional response to aging and caloric restriction in heart and adipose tissue. Aging Cell 6(5):673–688. doi:10.1111/j.1474-9726.2007.00319.x

Lorenz DR, Cantor CR, Collins JJ (2009) A network biology approach to aging in yeast. Proc Natl Acad Sci U S A 106(4):1145–1150. doi:10.1073/pnas.0812551106

Martin GS (2001) The hunting of the Src. Nat Rev Mol Cell Biol 2(6):467–475. doi:10.1038/3507309435073094

McCarter R, Masoro EJ, Yu BP (1985) Does food restriction retard aging by reducing the metabolic rate? Am J Physiol 248(4 Pt 1):E488–E490

Molina TJ, Kishihara K, Siderovski DP, van Ewijk W, Narendran A, Timms E, Wakeham A, Paige CJ, Hartmann KU, Veillette A et al (1992) Profound block in thymocyte development in mice lacking p56lck. Nature 357(6374):161–164. doi:10.1038/357161a0

Mootha VK, Lindgren CM, Eriksson KF, Subramanian A, Sihag S, Lehar J, Puigserver P, Carlsson E, Ridderstrale M, Laurila E, Houstis N, Daly MJ, Patterson N, Mesirov JP, Golub TR, Tamayo P, Spiegelman B, Lander ES, Hirschhorn JN, Altshuler D, Groop LC (2003) PGC-1alpha-responsive genes involved in oxidative phosphorylation are coordinately downregulated in human diabetes. Nat Genet 34(3):267–273. doi:10.1038/ng1180ng1180

Newman MEJ (2005) A measure of betweenness centrality based on random walks. Soc Network 27(1):39–54. doi:10.1016/j.socnet.2004.11.009

Park S, Komatsu T, Hayashi H, Yamaza H, Chiba T, Higami Y, Kuramoto K, Shimokawa I (2008) Calorie restriction

initiated at a young age activates the Akt/PKC zeta/lambda-Glut4 pathway in rat white adipose tissue in an insulin-independent manner. Age (Dordr) 30(4):293–302. doi:10.1007/s11357-008-9071-2

Peri S, Navarro JD, Amanchy R, Kristiansen TZ, Jonnalagadda CK, Surendranath V, Niranjan V, Muthusamy B, Gandhi TK, Gronborg M, Ibarrola N, Deshpande N, Shanker K, Shivashankar HN, Rashmi BP, Ramya MA, Zhao Z, Chandrika KN, Padma N, Harsha HC, Yatish AJ, Kavitha MP, Menezes M, Choudhury DR, Suresh S, Ghosh N, Saravana R, Chandran S, Krishna S, Joy M, Anand SK, Madavan V, Joseph A, Wong GW, Schiemann WP, Constantinescu SN, Huang L, Khosravi-Far R, Steen H, Tewari M, Ghaffari S, Blobe GC, Dang CV, Garcia JG, Pevsner J, Jensen ON, Roepstorff P, Deshpande KS, Chinnaiyan AM, Hamosh A, Chakravarti A, Pandey A (2003) Development of human protein reference database as an initial platform for approaching systems biology in humans. Genome Res 13(10):2363–2371. doi:10.1101/gr.168080313/10/2363

Pugh TD, Oberley TD, Weindruch R (1999) Dietary intervention at middle age: caloric restriction but not dehydroepiandrosterone sulfate increases lifespan and lifetime cancer incidence in mice. Cancer Res 59(7):1642–1648

Rangaraju S, Hankins D, Madorsky I, Madorsky E, Lee WH, Carter CS, Leeuwenburgh C, Notterpek L (2009) Molecular architecture of myelinated peripheral nerves is supported by calorie restriction with aging. Aging Cell 8 (2):178–191. doi:10.1111/j.1474-9726.2009.00460.x

Seddon B, Legname G, Tomlinson P, Zamoyska R (2000) Long-term survival but impaired homeostatic proliferation of naive T cells in the absence of p56lck. Science 290(5489):127–131

Sinclair DA (2005) Toward a unified theory of caloric restriction and longevity regulation. Mech Ageing Dev 126(9):987–1002. doi:10.1016/j.mad.2005.03.019

Spindler SR, Dhahbi JM, Mote PL (2003) Protein turnover, energy metabolism, aging, and caloric restriction. In: Mattson MP (ed) Advances in cell aging and gerontology, vol 14. Elsevier, Amsterdam, pp 69–86

Stichel CC, Luebbert H (2007) Inflammatory processes in the aging mouse brain: participation of dendritic cells and T-cells. Neurobiol Aging 28(10):1507–1521. doi:10.1016/j.neurobiolaging.2006.07.022

Straus DB, Weiss A (1992) Genetic evidence for the involvement of the lck tyrosine kinase in signal transduction through the T cell antigen receptor. Cell 70(4):585–593

Sung B, Park S, Yu BP, Chung HY (2004) Modulation of PPAR in aging, inflammation, and calorie restriction. J Gerontol A Biol Sci Med Sci 59(10):997–1006

Taylor IW, Linding R, Warde-Farley D, Liu Y, Pesquita C, Faria D, Bull S, Pawson T, Morris Q, Wrana JL (2009) Dynamic modularity in protein interaction networks predicts breast cancer outcome. Nat Biotechnol 27(2):199–204. doi:10.1038/nbt.1522

Trobridge PA, Levin SD (2001) Lck plays a critical role in Ca(2+) mobilization and CD28 costimulation in mature primary T cells. Eur J Immunol 31(12):3567–3579. doi:10.1002/1521-4141(200112)31:12<3567::AID-IMMU3567>3.0.CO;2-M [pii]10.1002/1521-4141(200112)31:12<3567::AID-IMMU3567>3.0.CO;2-M

Tusher VG, Tibshirani R, Chu G (2001) Significance analysis of microarrays applied to the ionizing radiation response. Proc Natl Acad Sci U S A 98(9):5116–5121. doi:10.1073/pnas.091062498091062498

Weindruch R, Keenan KP, Carney JM, Fernandes G, Feuers RJ, Floyd RA, Halter JB, Ramsey JJ, Richardson A, Roth GS, Spindler SR (2001) Caloric restriction mimetics: metabolic interventions. J Gerontol A Biol Sci Med Sci 56(Spec No 1):20–33

Xue H, Xian B, Dong D, Xia K, Zhu S, Zhang Z, Hou L, Zhang Q, Zhang Y, Han JD (2007) A modular network model of aging. Mol Syst Biol 3:147. doi:10.1038/msb4100189

Yu BP (1996) Aging and oxidative stress: modulation by dietary restriction. Free Radic Biol Med 21(5):651–668

Yu J, Yu T, Han J (2005) Aging-related changes in the transcriptional profile of cerebrum in senescence-accelerated mouse (SAMP10) is remarkably retarded by acupuncture. Acupunct Electrother Res 30(1–2):27–42

Yu H, Kim PM, Sprecher E, Trifonov V, Gerstein M (2007) The importance of bottlenecks in protein networks: correlation with gene essentiality and expression dynamics. PLoS Comput Biol 3(4):e59. doi:10.1371/journal.pcbi.0030059

Zhang L, Conejo-Garcia JR, Katsaros D, Gimotty PA, Massobrio M, Regnani G, Makrigiannakis A, Gray H, Schlienger K, Liebman MN, Rubin SC, Coukos G (2003) Intratumoral T cells, recurrence, and survival in epithelial ovarian cancer. N Engl J Med 348(3):203–213. doi:10.1056/NEJMoa020177348/3/203

Zou Y, Jung KJ, Kim JW, Yu BP, Chung HY (2004) Alteration of soluble adhesion molecules during aging and their modulation by calorie restriction. FASEB J 18(2):320–322. doi:10.1096/fj.03-0849fje03-0849fje